J Mol Med
DOI 10.1007/s00109-012-0911-2

ORIGINAL ARTICLE

A novel *COCH* mutation associated with autosomal dominant nonsyndromic hearing loss disrupts the structural stability of the vWFA2 domain

Hyun-Ju Cho · Hong-Joon Park · Maria Trexler · Hanka Venselaar · Kyu-Yup Lee · Nahid G. Robertson · Jeong-In Baek · Beom Sik Kang · Cynthia C. Morton · Gert Vriend · László Patthy · Un-Kyung Kim

Received: 13 December 2011 / Revised: 10 April 2012 / Accepted: 30 April 2012

Abstract Mutations in *COCH* have been associated with autosomal dominant nonsyndromic hearing loss (DFNA9) and are frequently accompanied by vestibular hypofunction. Here, we report identification of a novel missense mutation, p.F527C, located in the vWFA2 domain in members of a Korean family with late-onset and progressive hearing loss. To assess the molecular characteristics of this cochlin mutant, we constructed both wild-type and mutant cochlin constructs and transfected these into mammalian cell lines. Results of immunocytochemistry analysis demonstrated localization of the cochlin mutant in the endoplasmic reticulum/Golgi complex, whereas western blot analyses of cell lysates revealed that the mutant cochlin tends to form covalent complexes that are retained in the cell. Biochemical analyses of recombinant vWFA2 domain of cochlin carrying the p.F527C mutation revealed that the mutation increases propensity of the protein to form covalent disulfide-bonded dimers and affects the structural stability but not the collagen-affinity of the vWFA2 domain. We suggest that the instability of mutant cochlin is the major driving force for cochlin aggregation in the inner ear in DFNA9 patients carrying the *COCH* p.F527C mutation.

Keywords Nonsyndromic hearing loss · DFNA9 · Cochlin · Mutation · Protein stability

Hyun-Ju Cho and Hong-Joon Park contributed equally to this work.

Electronic supplementary material The online version of this article (doi:10.1007/s00109-012-0911-2) contains supplementary material, which is available to authorized users.

H.-J. Cho · J.-I. Baek · U.-K. Kim (✉)
Department of Biology, College of Natural Sciences,
Kyungpook National University,
Daegu 702-701, South Korea
e-mail: kimuk@knu.ac.kr

H.-J. Park
Soree Ear Clinics,
Seoul, South Korea

M. Trexler · L. Patthy (✉)
Institute of Enzymology, Biological Research Center,
Hungarian Academy of Sciences,
Budapest, Hungary
e-mail: patthy@enzim.hu

H. Venselaar · G. Vriend
Radboud University Nijmegen Medical Centre,
Nijmegen, The Netherlands

K.-Y. Lee
Department of Otorhinolaryngology-Head and Neck Surgery,
College of Medicine, Kyungpook National University,
Daegu, South Korea

N. G. Robertson · C. C. Morton
Department of Obstetrics, Gynecology and Reproductive Biology,
Brigham and Women's Hospital, Harvard Medical School,
Boston, MA, USA

B. S. Kang
School of Life Science and Biotechnology,
Kyungpook National University,
Daegu 702-701, South Korea

C. C. Morton
Department of Pathology, Brigham and Women's Hospital,
Harvard Medical School,
Boston, MA, USA

Published online: 19 May 2012

Introduction

Autosomal dominant nonsyndromic hearing loss (ADNSHL) accounts for ~20 % of genetic hearing impairments, and 25 causative genes have been identified to date (http://hereditaryhearingloss.org). Mutations in *COCH* are causative for DFNA9 [1].

The product of the *COCH* gene, cochlin is an extracellular protein that is mainly expressed in the inner ear and is found at low levels in eye, cerebellum, liver, and kidney [2]. It consists of an N-terminal secretory signal peptide, a Limulus factor C, cochlin, and late gestation lung protein, Lgl1 (LCCL) domain, and two von Willebrand factor A (vWFA) domains. The LCCL module is an autonomously folded domain found in various metazoan proteins [3]. vWFA domains are present in several major components of the extracellular matrix, suggesting that cochlin may play a structural role in the extracellular matrix of the cochlea [1, 2].

To date, DFNA9 patients have been identified in 32 families; each family has a different *COCH* mutation, but all are associated with common clinical features [4–6]. The families have late-onset progressive hearing loss. The age of onset varies from 20 to 90 years, and the symptoms begin with high-frequency hearing loss. As with other DFNA patients, hearing loss deteriorates with age and expands to all frequencies. Some, but not all, patients experience other symptoms specific to DFNA9, including vestibular dysfunctions such as vertigo and tinnitus [5]; it must be emphasized, however, that vertigo may be caused by mutations in genes other than the *COCH* gene [7]. Furthermore, in histopathological studies, affected individuals were found to have mucopolysaccharide deposits in the spiral ligament, spiral limbus, channels of the cochlear and vestibular nerves, and stroma underlying the vestibular epithelia. These eosinophilic acellular materials have been suggested to result from an accumulation of misfolded mutant cochlin, either alone or in combination with other molecules [1, 8, 9]. In this study, we identified a novel mutation involving a cysteine residue in the vWFA2 domain that likely causes structural instability and anomalies, and we investigated the molecular characteristics of this cochlin mutant.

Materials and methods

Subjects and clinical diagnosis

A Korean family with late-onset progressive hearing loss was recruited from the Department of Otorhinolaryngology-Head and Neck Surgery, Ajou University, Suwon, Korea. A total of five individuals, including two affected and three unaffected members, participated in this study (Fig. 1a). After physical and otoscopic examinations, pure tone audiometry (PTA) was performed in a sound-conditioned room, and the averages of the hearing thresholds at 0.25, 0.5, 1, 2, 4, and 8 kHz were calculated. Vestibular function was assessed in the proband (III-9) by spontaneous nystagmus, head shaking test, Dix-Hall pike test, positional test, posturography, and rotation test. All participants provided written informed consent according to the protocol approved by the ethics committee of the Institutional Review Board of the Ajou University College of Medicine prior to the study. One hundred unrelated individuals were tested with PTA to exclude hearing loss, and used as normal controls.

Fig. 1 Novel *COCH* mutation p.F527C identified in a Korean ADNSHL family. **a** The Korean SD-39 pedigree showing autosomal dominant nonsyndromic hearing loss. **b** The patients have progressive hearing loss with damage to their hearing ability at high frequencies. **c** The p.F527C mutation was identified; this mutation substitutes thymine for guanine at nucleotide position 1580. **d** This novel mutation introduces a cysteine residue in the vWFA2 domain in place of phenylalanine, a residue conserved in cochlins of various vertebrate species

Genetic analysis

Genomic DNA was extracted from the peripheral blood of the five family members and of 100 unrelated normal controls using a FlexiGene DNA extraction kit (Qiagen, Hilden, Germany). All 12 exons and flanking intronic sequences of *COCH* (GenBank accession no. NM_004086) were amplified by polymerase chain reaction (PCR) and subsequently sequenced using an ABI PRISM Big Dye Terminator Cycle Sequencing Kit (v.3.1) and an ABI PRISM3130XL DNA analyzer (Applied Biosystems, Foster City, CA) (Supplementary Table 1). ABI Sequencing Analysis (v.5.0) and Lasergene–SeqMan software were used for data analysis. When an identified sequence variant segregated with the phenotype within the family, the presence of the variant was evaluated by sequencing of genomic DNA from 100 unrelated Korean subjects with normal hearing.

Mammalian expression of full-length cochlin

The human wild-type *COCH* expression construct in a pcDNA3 vector with three C-terminal hemagglutinin (HA) epitope tags [10] was used to express human wild-type cochlin. To investigate the functional characteristics of the cochlin mutant, p.F527C was introduced into the wild-type construct using the QuikChange site-directed mutagenesis kit (Stratagene Inc., La Jolla, CA). Three previously identified mutations, p.W117R, p.M512T, and p.C542Y, were also constructed as experimental controls. Each of the mutant and wild-type *COCH* constructs were transiently transfected into HeLa cells, HEK-293 cells or C3H10T½ cells using the Lipofectamine 2000 transfection reagent (Invitrogen, Carlsbad, CA) according to the manufacturer's instructions.

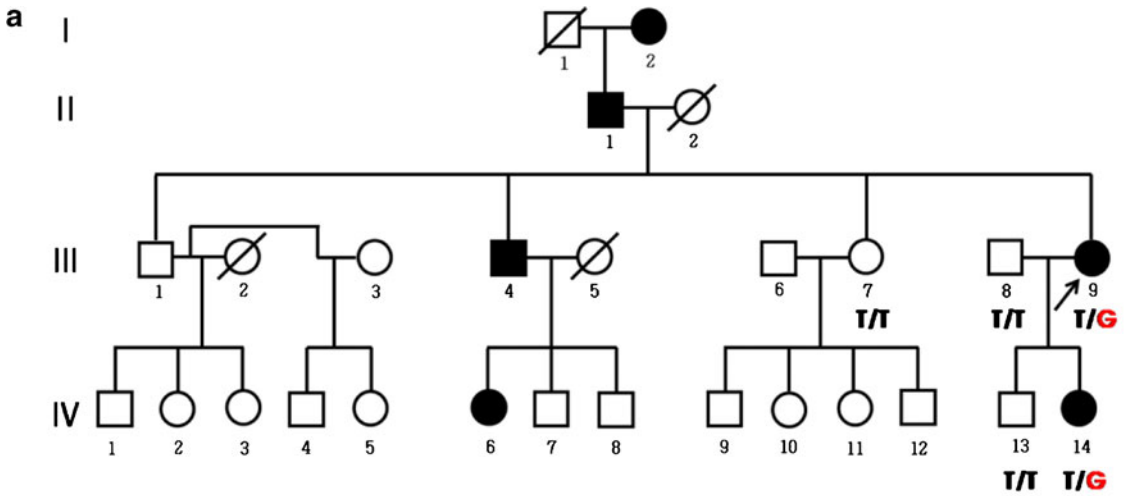
a
I
II
III
IV
1
2
3
4
5
6
7
8
9
10
11
12
13
14
T/T
T/G
T/T
T/G

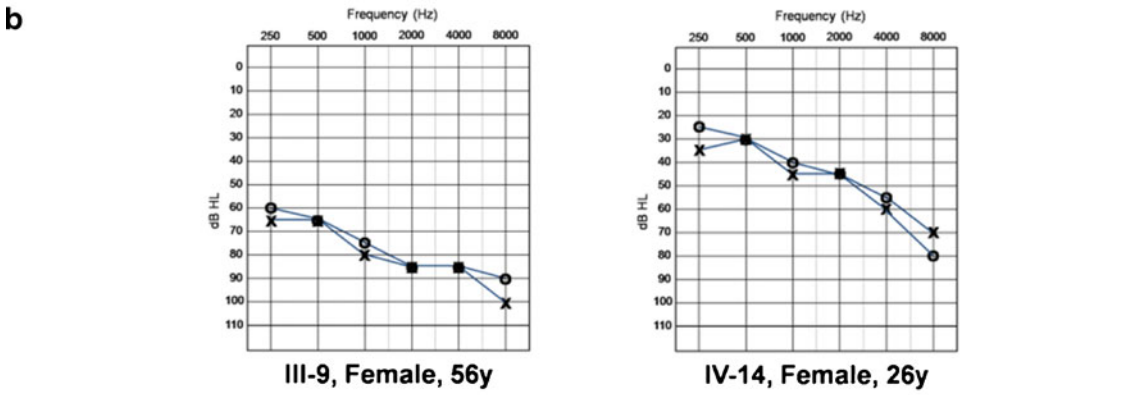
b
Frequency (Hz)
250
500
1000
2000
4000
8000
dB HL
III-9, Female, 56y
IV-14, Female, 26y

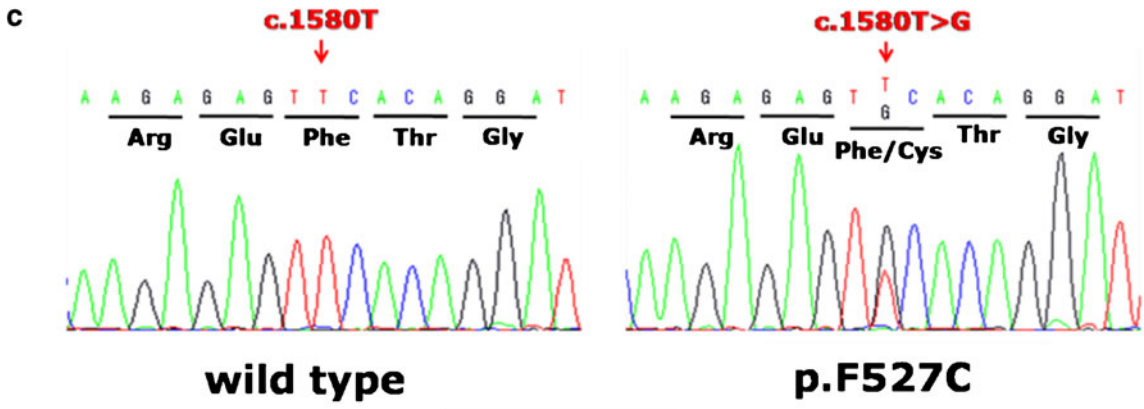
c
c.1580T
c.1580T>G
A A G A G A G T T C A C A G G A T
Arg
Glu
Phe
Thr
Gly
A A G A G A G T T C A C A G G A T
G
Arg
Glu
Phe/Cys
Thr
Gly
wild type
p.F527C

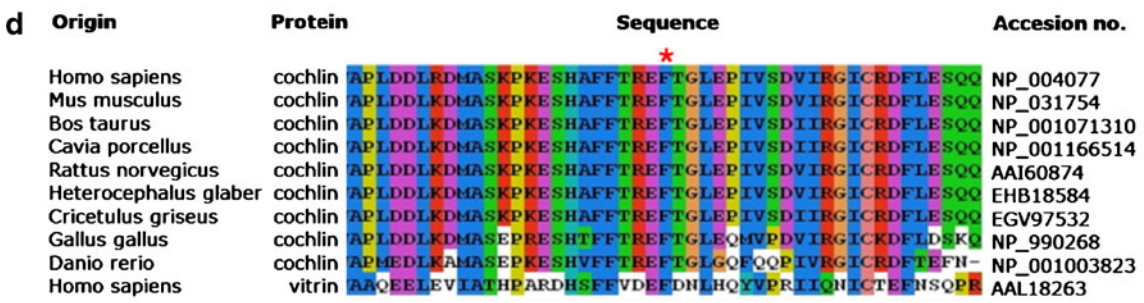
d
Origin
Protein
Sequence
Accesion no.
Homo sapiens cochlin NP_004077
Mus musculus cochlin NP_031754
Bos taurus cochlin NP_001071310
Cavia porcellus cochlin NP_001166514
Rattus norvegicus cochlin AAI60874
Heterocephalus glaber cochlin EHB18584
Cricetulus griseus cochlin EGV97532
Gallus gallus cochlin NP_990268
Danio rerio cochlin NP_001003823
Homo sapiens vitrin AAL18263

Immunocytochemistry

Twenty-four hours after transfection, intracellular cochlin expressed by the wild-type and mutant *COCH* constructs was immunostained. Immunolabeling procedures were performed as previously described [11]. Rabbit anti-HA monoclonal antibody (Cell Signaling Technology, Danvers, MA) was used to label cochlin, and mouse anti-KDEL monoclonal antibody (Enzo Life Sciences, Farmingdale, NY) and mouse anti-human golgin-97 antibody (Invitrogen, Carlsbad, CA) were used to label the endoplasmic reticulum (ER) and Golgi complexes, respectively. Goat anti-rabbit Alexa555 (Zymed, San Francisco, CA) and goat anti-mouse Alexa488 (Zymed, San Francisco, CA) were used as secondary antibodies. Nuclei were counterstained with 4,6-diamidine-2-phenylindole dihydrochloride (DAPI), and the slides were visualized and the images captured using a Zeiss DE/AX10 Imager A1 fluorescence microscope system (Carl Zeiss, Oberkochen, Germany).

Immunoprecipitation and western blot analysis

Aliquots (250 μl) of culture medium from the transfected cells were immunoprecipitated using Dynabeads® Protein G (Invitrogen, Carlsbad, CA) and mouse anti-HA monoclonal antibody (clone HA.11; Covance, Princeton, NY). Both cell lysates and immunoprecipitated proteins were prepared in reducing and non-reducing conditions and separated by sodium dodecyl sulfate polyacrylamide gel electrophoresis (SDS-PAGE; 8 % gels) followed by immunoblotting, as previously described [12].

Protein modeling

YASARA's automatic homology modeling script was used to generate a model of the second vWFA domain in cochlin [13]. The model was based on PDB file 1JLM which contains the I domain from αM intergrin [14]. The sequence identity between the cochlin vWFA2 domain and 1JLM was 29 % over a length of 177 amino acids. More details, the model, and the analysis of the mutation are available at http://www.cmbi.ru.nl/~hvensela/cochlin.

Expression and biochemical characterization of the mutant vWFA2 domain (for deatails, see Electronic supplementary material).

Results

Clinical features and mutation analysis

Affected individuals of the SD39 family showed moderate-severe to profound bilateral sensorineural hearing loss with a downward sloping audiometric configuration indicating typical autosomal dominant hearing loss (Fig. 1b). The result of vestibular test of proband (III-9) did not show any vestibular dysfunctions. A total of 12 exons and flanking intron sequences of *COCH* in five members of the SD39 family were examined using PCR-amplified direct sequencing analysis. As a result of mutation screening of the *COCH* gene in the SD39 family, a missense mutation was detected in the two affected members who were heterozygous for the change of thymine to guanine at nucleotide position 1,580 (c.1580T>G) in exon 12 (Fig. 1c). This substitution leads to a change from the amino acid phenylalanine, a large, hydrophobic residue, to cysteine, a much smaller hydrophobic residue at position 527 (p.F527C). The phenylalanine residue is located in a region of the second vWFA domain of cochlin that is conserved among vertebrate homologs such as *Homo sapiens*, *Mus musculus*, *Bos taurus*, *Cavia porcellus*, *Rattus norvegicus*, *Heterocephalus glaber*, *Cricetulus griseus*, *Gallus gallus*, and *Danio rerio*, and in *H. sapiens vitrin* (Fig. 1d). Furthermore, this mutation showed complete co-segregation with hearing loss in the SD39 family; it was found only in the affected members and was absent in normal members of the pedigree (Fig. 1a). Additionally, the mutation did not exist in 100 unrelated normal control individuals, as diagnosed by the PTA test, and did not find in 1000 Genome database.

Effects of the p.F527C mutation on subcellular localization, secretion, and disulfide bond formation

To investigate the intracellular location and secretion of normal and mutant cochlin, we performed subcellular localizations of wild-type and mutant cochlins by immunocytochemistry. Intracellular wild-type cochlin in HeLa cells was strongly detected in the perinuclear region and showed a diffuse appearance throughout the cytoplasm (Fig. 2). Cochlin co-localized with the reticular formation of the ER from the nucleus to the membrane, and was observed more clearly with a compacted appearance in the Golgi body. Protein labeling showed the same patterns in HEI-OC1, HEK293, and C3H10T1/2 cells transfected with the wild-type *COCH* construct (data not shown). The p.F527C and three other mutant cochlin proteins showed localizations similar to that of wild-type, with strong fluorescent signals adjacent to the nucleus and gradually decreasing signals away from the nucleus, indicating that all the mutant cochlin proteins passed through the secretory pathway. One of the mutants tested, p.W117R, which had been previously investigated using the same method, was used as an experimental control, and the previous results were replicated [11]. Western blot analysis supported the immunocytochemistry results. In reducing conditions, all of the mutant cochlins from both cell lysates and conditioned media exhibited identical ~64 kDa bands that correspond to the size of

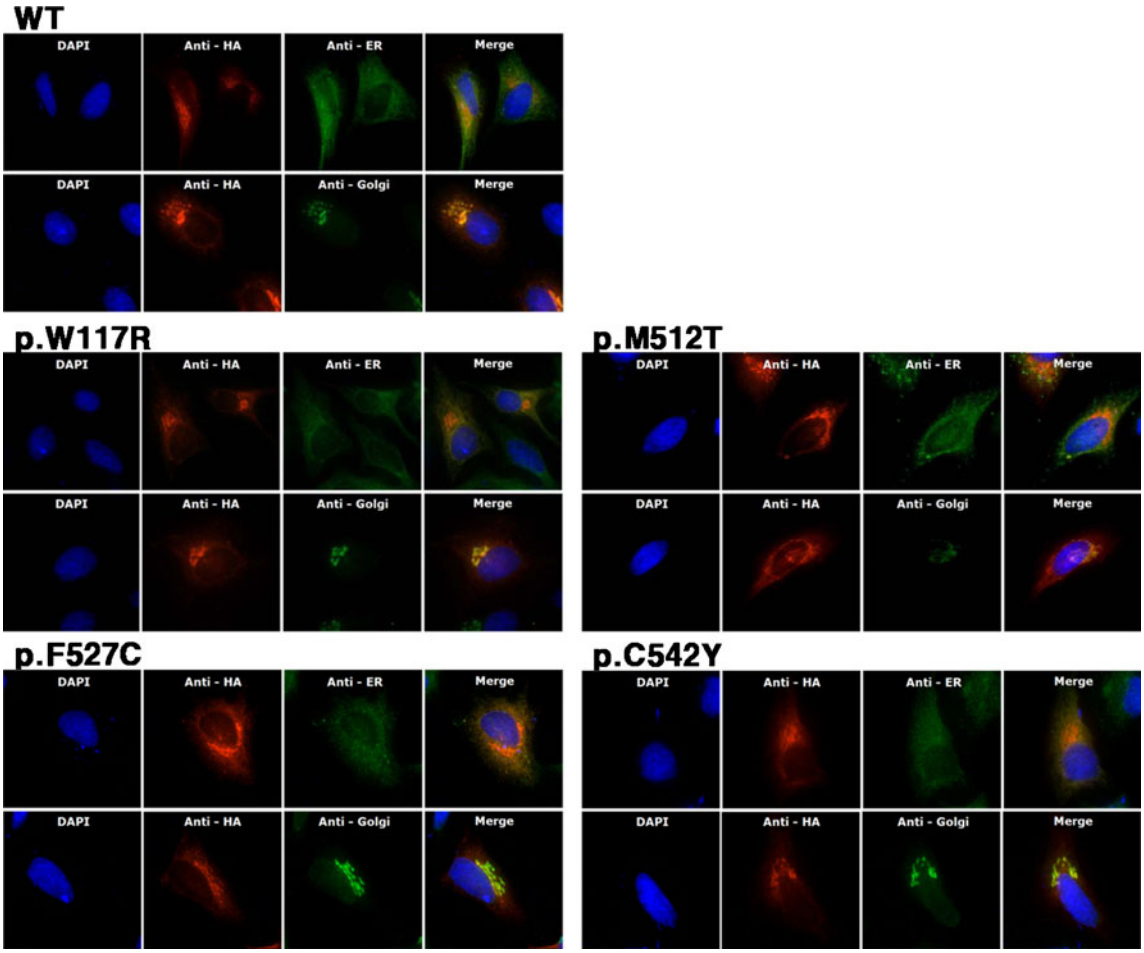

Fig. 2 Intracellular localization of wild-type and mutant cochlins in human HeLa cells. HA-tagged cochlin proteins expressed by transfected *COCH* constructs were detected by HA antibodies and were immunolabeled with Alexa 555 (*red*). KDEL antibody and Golgin-97 antibodies were used to target the ER and Golgi complex, respectively, and both were labeled with Alexa 488 (*green*). Nuclei were counterstained with DAPI (*cyan*). Double immunolabeling on the merged image shows the co-localization of cochlin and intracellular organelles

wild-type cochlin (Fig. 3). Cochlin migrated slightly faster in non-reducing conditions than in reducing conditions, suggesting that the disulfide bonds remained intact and that the proteins retained their tertiary folding.

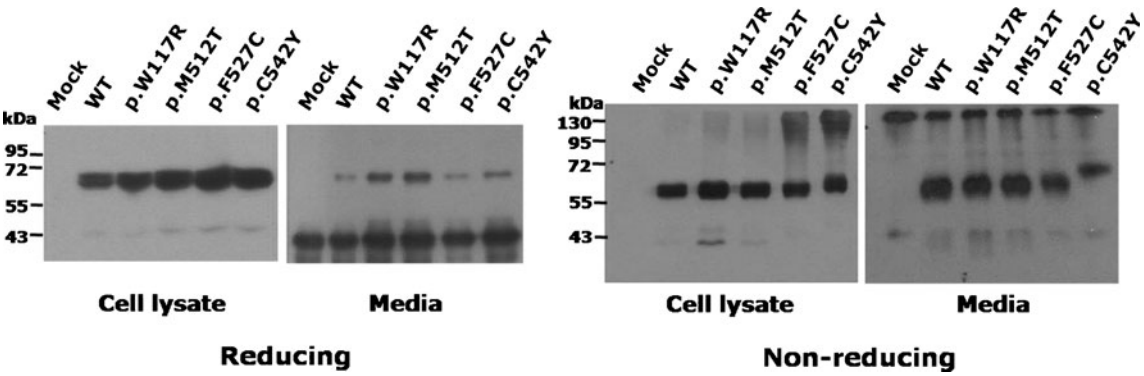

Fig. 3 Western blot analysis of intracellular and secreted cochlins in both reducing and non-reducing conditions. Intracellular cochlin proteins were harvested as whole-cell lysates and extracellular cochlin proteins were immunoprecipitated with anti-HA antibodies. Both cell lysates and immunoprecipitated proteins were prepared in reducing and non-reducing conditions and separated by SDS/PAGE in 8 % gels, followed by immunoblotting. Molecular weight is estimated from PageRuler Prestained Protein Ladder. The band with Mr of <43 kDa of media in reducing state is a heavy chain of mouse anti-HA monoclonal antibody used for immuno-precipitation; mouse anti-HA monoclonal antibody is present as ~130 kDa band in non-reducing state

In non-reducing conditions, cell lysates of wild-type, p.W117R and p.M512T cochlins contained only bands corresponding to monomeric protein, whereas in both p.F527C and p.C542Y, a large proportion of cochlin was found in bands of ≥130 kDa. This observation suggests that unpaired cysteines of the latter mutants promote the formation of covalent, disulfide bonded complexes. The high molecular weight complexes of p.F527C and p.C542Y cochlin, however, are not secreted as evidenced by the fact that these complexes are missing from the conditioned media (Fig. 3).

In non-reducing conditions, the p.C542Y mutant cochlin showed a band shift caused by slower migration, and the other mutant cochlin proteins, including p.F527C, migrated similarly to the wild-type. These results suggest that the p.C542Y mutation disrupts the formation of normal intracellular disulfide bonds and in the other mutants, including p.F527C, disulfide bridges do not appear to be disrupted.

Protein modeling

The novel mutation p.F527C introduces a new cysteine in the vWFA2 domain, and the presence of this extra, unpaired cysteine was found to promote formation of covalent, disulfide bonded complexes. To investigate the effect of this mutation on protein structure more closely, we performed protein modeling and protein structure analyses.

The 3D homology model of the cochlin vWFA2 domain was obtained using the structure of I domain from αM integrin, with a 29 % amino acid sequence identity to vWFA2, as a template (PDB file 1JLM) [14]. Similar to other vWFA domains, the vWFA2 of cochlin has the structure as the central beta-sheet of six strands, flanked by three and four helices (Fig. 4a). It also has a perfectly conserved metal ion-dependent adhesion site motif, which has an important role in structural stability and ligand binding in vWFA domain-containing proteins [15–19].

The I domain of integrin, the template protein for this study, has been observed in two conformations: the closed form (PDP ID; 1JLM) and the open form (PDP ID; 1IDO) [14, 20, 21]. The major conformational change from the closed form to the open form is that the F302 residue is buried in a hydrophobic pocket in the closed form, whereas it is exposed in the open form [22]. The modeled structure of the vWFA2 domain of cochlin was similar to the closed form of integrin. Interestingly, the F527 residue of cochlin aligned with the F302 of αM integrin (PDB ID; 1IDO), the residue showing the predominant alteration in the integrin structure. In the wild-type, F527 is located in the loop region preceded by the C-terminal helix and interacts with other hydrophobic residues (Fig. 4b). However, the F527C mutation places the cysteine residue in this specific location, and the hydrophobic interactions of the loop following α7 with the surrounding hydrophobic residues are eliminated (see the web site for more detail, http://www.cmbi.ru.nl/~hvensela/cochlin). This breakdown of the native hydrophobic interactions could lead to a conformational change in the cochlin vWFA2 domain, resulting in a conformation that is similar to the open form of the I domain of integrin.

Analysis of the vWFA2 domain of human cochlin carrying the p.F527C mutation

Ni-affinity chromatography of the culture media of *Pichia pastoris* transformed with the pPICZαA-vWFA2_F527C expression vector confirmed that the cells secreted the mutant vWFA2 domain of cochlin. However, the amount was lower than that observed in the case of the wild-type protein under the same conditions; the yield was 12 mg/l for the wild-type protein, whereas it was 3.7 mg/l for the mutant protein, suggesting that it may not be secreted as efficiently as wild-type.

SDS-PAGE analysis of the fractions isolated by Ni-affinity chromatography revealed that under non-reducing conditions, ~50 % of the protein was present in a band with approximately the same molecular mass (22 kDa) as the wild-type coch_vWFA2 protein (compare coch_vWFA2 and coch_vWFA2_F527C in non-reducing condition in Fig. 5). A major difference between mutant and wild-type proteins is that this band was diffuse in the case of the mutant protein, suggesting structural heterogeneity of the monomer. Another major difference between wild-type and mutant proteins was that under non-reducing conditions, ~50 % of the mutant protein was present in a band with an apparent molecular mass

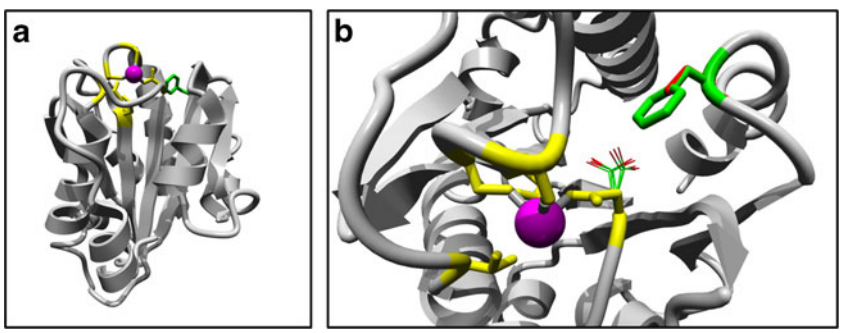

Fig. 4 Protein modeling of the vWFA2 domain containing the p.F527C mutation. An overview of the complete model (**a**) and a close-up of the mutation (**b**). A homology model of the vWFA2 domain was computed using the structure of the I domain of αM integrin as a template

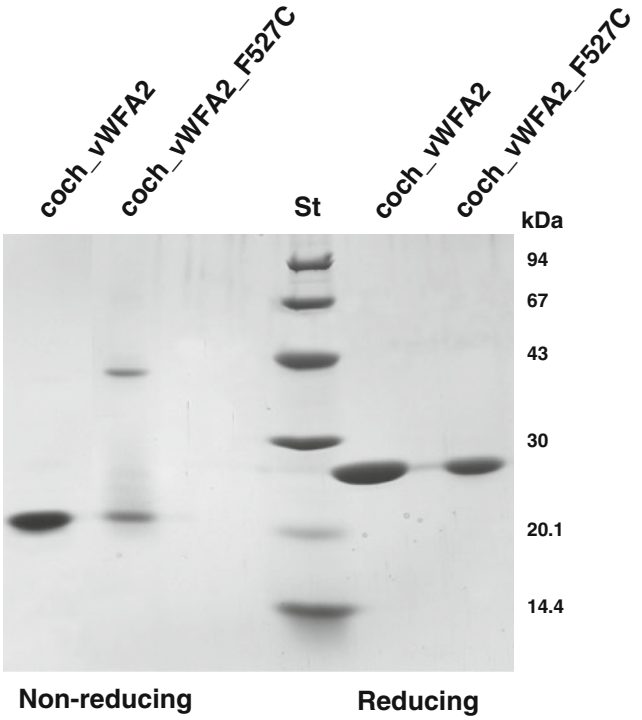

Fig. 5 SDS-PAGE analysis of the wild-type and p.F527C mutant vWFA2 domains of human cochlin. Coch_vWFA2 and coch_vWFA2_F527C proteins were isolated by affinity chromatography on Ni Sepharose. *St* the pattern of the Low Molecular Weight Calibration Kit (Amersham Pharmacia Biotech, Uppsala, Sweden)

of ~44 kDa, suggesting formation of covalent dimers (compare coch_vWFA2 and coch_vWFA2_F527C in non-reducing condition in Fig. 5). Because both wild-type and mutant proteins were present in single bands under reducing conditions with an apparent molecular mass of ~25 kDa (see coch_vWFA2 and coch_vWFA2_F527C in reducing condition in Fig. 5), we concluded that the monomeric forms unique to the mutant protein are folding variants with a non-native 3D structure and that the mutant dimer is connected by intermolecular disulfide bond(s). Unless otherwise indicated, we used the monomeric form of the coch_vWFA2_F527C protein for structural and functional characterization.

Structural characterization of the vWFA2 domain of human cochlin carrying the p.F527C mutation

The N-terminal amino acid sequence of the secreted mutant protein was found to be *EAEAEF***SKTCYNS**; residues of the second vWFA domain of cochlin are highlighted in bold, and residues in italics originated from the vector. The structural integrity of the mutant vWFA2 domain was analyzed by CD spectroscopy. The circular dichroism spectrum of the coch_vWFA2_F527C protein was similar to that of the wild-type coch_vWFA2 domain [23] in showing the characteristic large negative ellipticity between 210 and 225 nm with a small trough between these wavelengths, although the minimum at 210 nm is deeper for the mutant (compare Fig. 6a, b). The thermal unfolding of coch_vWFA2_F527C was characterized by monitoring the effect of heating on changes in the CD signal at 222 nm. In contrast to the wild-type coch_vWFA2 protein, where thermal unfolding shows a single, sharp transition with a T_m value of 52 °C, the transition of the mutant protein was broad, and derivation of the curve showed that thermal unfolding is characterized by several T_m values (compare Fig. 7a, b).

The most likely explanation for the combined data obtained by SDS-PAGE analysis and CD spectroscopy is that although the 3D structure of the mutant monomeric protein is native like, as reflected in the similarity of the wild-type and mutant forms with respect to the CD spectra recorded at 195–250 nm, not all forms have the disulfide bonds characteristic of the wild-type protein, which is reflected in the structural heterogeneity of the monomer observed with SDS-PAGE under non-reducing conditions. In addition, these forms are less stable than the wild-type, which is reflected by the fact that the majority of them denature at T_m values lower than that of the wild-type.

Characterization of the interaction of type II collagen with the vWFA2 domain of human cochlin carrying the p.F527C mutation

Surface plasmon resonance studies of the coch_vWFA2_F527C protein revealed that the mutant monomeric protein bound to collagen type II immobilized on the surface of the sensor chip (Fig. 8a). Analysis of the sensorgrams, however, revealed that in contrast with the wild-type protein, which yielded good fits with the simple model of a 1:1 Langmuir interaction, the association and dissociation curves of the interaction of the mutant protein could not be fitted to this simple model.

Because the monomeric mutant protein used in this study as an analyte was found to contain folding variants, the majority of which denature at lower temperatures than the wild-type (see above), we used a model in which we assumed that the monomeric preparation has components that may differ in affinity for type II collagen. This model of the heterogeneous analyte gave acceptable fits if we assumed the presence of two species in a ratio of 9:1 and that the major species had a weaker affinity for type II collagen ($K_d=1.4\times10^{-5}$ M) than the minor species ($K_d=2.9\times10^{-7}$ M). It should be noted that the affinity of the minor species for type II collagen is comparable to that observed in the case of the wild-type protein ($K_d=9.45\times10^{-8}$ M) [23]. It seems likely that the component with a collagen affinity comparable to that of the wild-type protein corresponds to the folding variant that denatures at a T_m of 52.5 °C (see

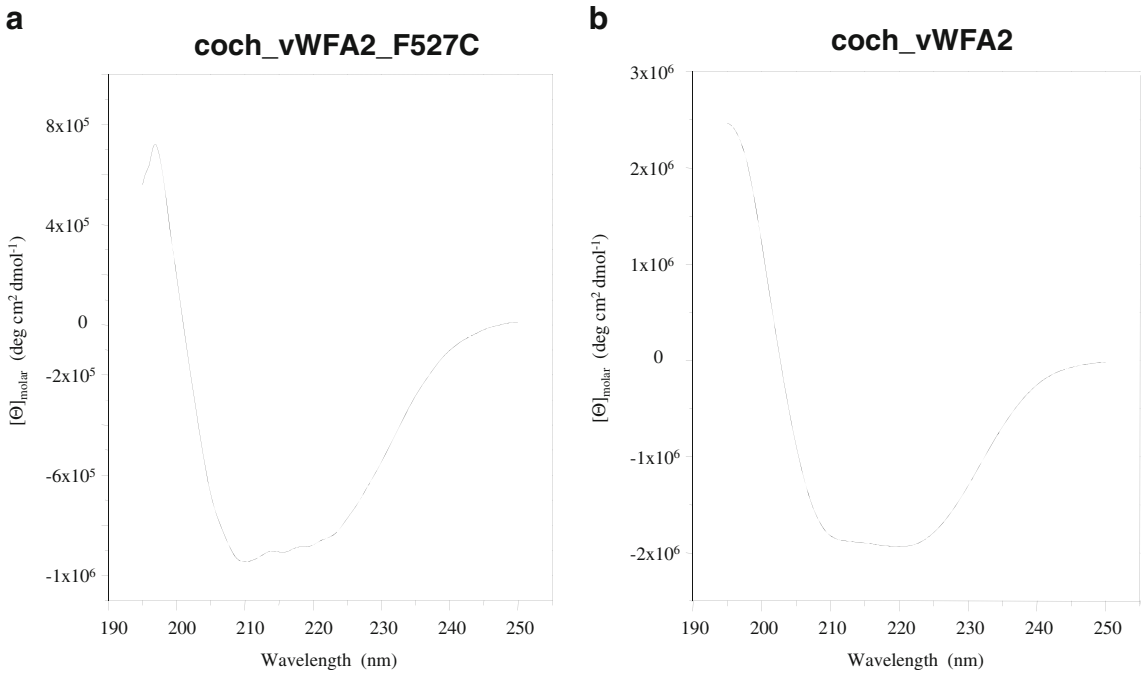

Fig. 6 Comparison of the circular dichroism spectra of the wild-type and p.F527C mutant vWFA2 domains of human cochlin. **a** Far-ultraviolet circular dichroism spectra of the recombinant coch_vWFA2_F527C protein. **b** Far-ultraviolet circular dichroism spectra of the recombinant wild-type coch_vWFA2 protein

Fig. 7a). The fact that the mutation is compatible with a high affinity for type II collagen indicates that the phenylalanine residue affected by the p.F527C mutation has no direct role in collagen binding.

However, because the coch_vWFA2_F527C protein shows a significant propensity to form covalent dimers (see Fig. 5), it is important to examine whether the collagen binding site is accessible in the dimer. Experiments with the dimeric form of

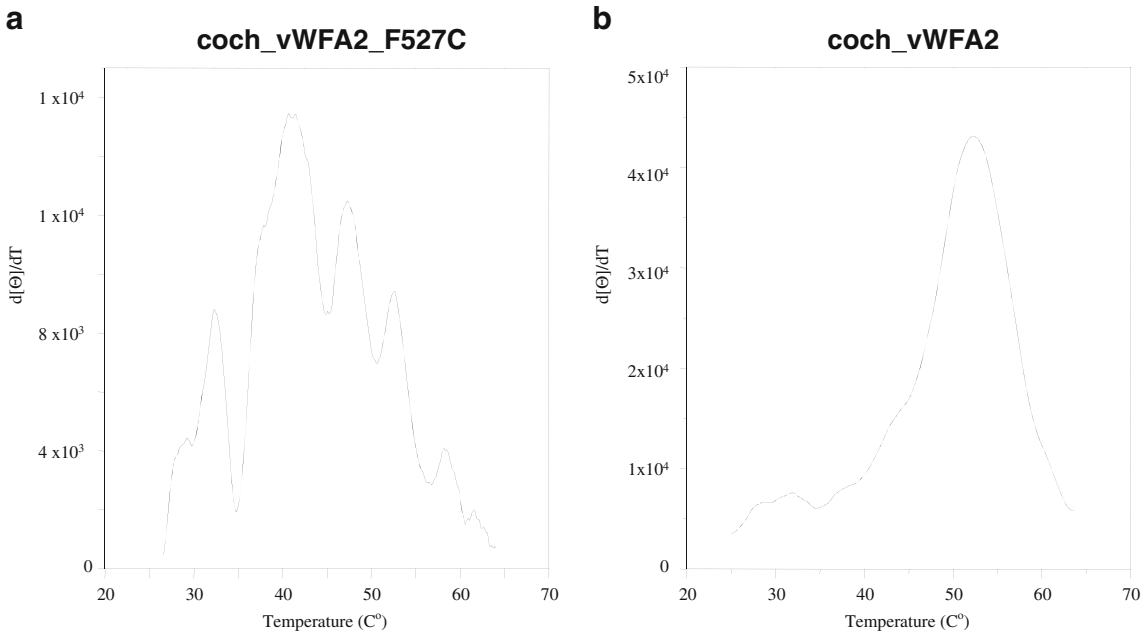

Fig. 7 Comparison of the temperature-dependence of the CD spectra of the wild-type and p.F527C mutant vWFA2 domains of human cochlin. **a** Changes in the CD spectra of the recombinant coch_vWFA2_F527C protein. **b** Changes in the CD spectra of recombinant wild-type coch_vWFA2 protein (reproduced from Nagy et al. [23]). Changes in the CD spectra of the proteins were monitored at 222 nm in 10 mM Tris–HCl buffer, pH 8.0, during the course of heating from 20 to 90 °C at a rate of 50 °C/h. Melting temperatures were determined by derivative processing using the Spectral Analysis program for Windows 95/NT version 1.53.04 (JASCO)

the coch_vWFA2_F527C protein revealed that it also shows high affinity for type II collagen (Fig. 8b). Analysis of the sensorgrams gave an acceptable fit to the model of the heterogeneous analyte if the presence of two species is assumed to be in a ratio of 1:1, where one of the species had a relatively weak affinity for type II collagen (K_d=6.1×10^{-6} M) and the other component had a higher affinity (K_d=9.5×10^{-7} M). The observation that the dimer of coch_vWFA2_F527C protein also has high affinity for type II collagen (Fig. 8b) suggests that the DFNA9 phenotype observed in the case of patients carrying this mutation is not due to loss of collagen affinity.

Discussion

In the present study, we identified a novel *COCH* mutation, p.F527C, that causes autosomal dominant nonsyndromic hearing loss in a Korean family. This mutation is located in the vWFA2 domain and introduces a cysteine residue into the protein.

We performed functional analyses with both full-length cochlin and the vWFA2 domain of cochlin containing this novel mutation to identify structural or functional characteristics that could shed light on the pathology of the mutant cochlin. The overall conclusion from studies on full-length cochlin is that the p.F527C mutant is expressed and secreted in the media; however, a significant proportion of the protein forms covalent complexes that are retained in the cell. In the case of the recombinant vWA2 domain of cochlin carrying this mutation (coch_vWFA2_F527C protein), it was clear that the p.F527C mutation resulted in a significant destabilization of the structure of the domain and increased propensity to form covalent disulfide-bonded dimers.

To gain further insight into the structural consequences of the p.F527C mutation, we predicted the 3D structure of the cochlin vWFA2 domain with the YASARA's automatic homology modeling script [24] using the crystal structure of the I domain of αM integrin as a template. These experiments have shown that the vWFA2 domain of cochlin adopts a conformation similar to the closed form of the I domain of integrin by maintaining the hydrophobic interactions of F527. However, the p.F527C mutation affects these hydrophobic interactions leading to a transition to a conformational state similar to that characteristic of the open form of the I domain of integrin. This structural change decreases the stability of the protein, explaining why the recombinant coch_vWFA2_F527C protein is characterized by lower T_m values than the wild-type. It seems likely that this instability is a major cause of cochlin aggregation and polymer formation in the inner ear in DFNA9 patients.

Analyses of the affinity of coch_vWFA2_F527C protein for collagen type II have revealed that the p.F527C mutation did not eliminate binding, indicating that the affected F527 residue of vWFA2 has no direct role in collagen binding. Based on these results, we hypothesize that the p.F527C mutation of cochlin causes DFNA9 phenotype through cochlin aggregation, rather than through loss of function of the protein. This model implies that the p.F527C mutant cochlin has dominant-negative effects on the hearing functionality of DFNA9 patients and is consistent with the inheritance pattern of our DFNA9 pedigree with this mutation and with the finding of hearing loss in *Coch*$^{G88E/+}$ heterozygotes and not in *Coch*$^{-/+}$ heterozygotes, reflecting that the mutation's deleterious effects are likely not the result of haploinsufficiency [25].

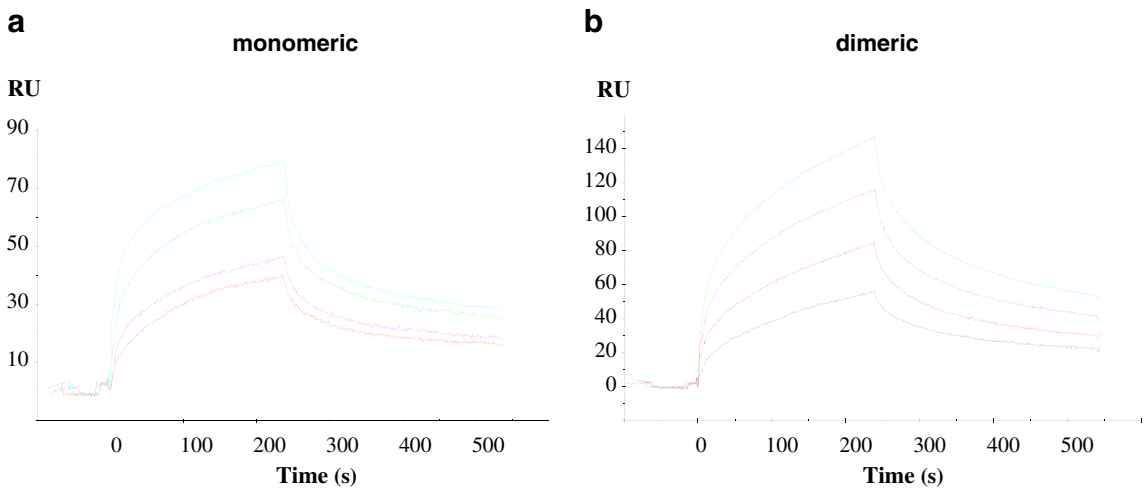

Fig. 8 Characterization of the interaction of the coch_vWFA2_F527C protein with type II human collagen by surface plasmon resonance assays. **a** Sensorgrams of the interactions of monomeric coch_vWFA2_F527C protein (1, 2, 5, and 10 μM) with immobilized type II human collagen. **b** Sensorgrams of the interactions of dimeric coch_vWFA2_F527C protein (500 nM, 1.5 μM, 2.5 μM, and 3 μM) with immobilized type II human collagen

In view of the fact that the late-onset age of DFNA9 patients is related to accumulation of the negative effects of harboring this unstable protein, differences in accumulation rates among the patients likely lead to various ages of onset for DFNA9, ranging from the second to ninth decades. Until now, how the body reacts to aggregated mutant cochlin and causes hearing loss has not been clear. We hypothesize that the mucopolysaccharide deposits induce an autoimmune response and results in tissue degeneration. Supporting this hypothesis, autoimmune sensorineuronal hearing loss has been associated with auto-antibodies to cochlin [26, 27] as well as increased frequencies of cochlin-specific T cells [28].

In three Dutch families carrying p.Pro51Ser and p.Gly88-Glu mutations in the *COCH* gene, a peculiar pattern of midlife onset vertical corneal striae was observed, suggesting a significant association between this phenotype and mutations in the *COCH* gene [29]. The DFNA9 family investigated in this study showed only the clinical symptoms of hearing loss; however, most other patients with the *COCH* mutation suffer hearing loss accompanied by vestibular dysfunction. Further studies on the relationship of these different clinical features and the type of mutation in patients with *COCH* gene defects are needed.

Acknowledgments This work was supported by Basic Science Research Program through the National Research Foundation of Korea (NRF) funded by the Ministry of Education, Science and Technology (2009-0087615) to U.-K.K, by National Scientific Research Fund of Hungary (OTKA) grant 75836 to L.P., and by the National Institutes of Health RO1 DC03402 to C.C.M.

Conflict of interest statement The author(s) declare that they have no competing interests.

References

1. Robertson NG, Lu L, Heller S, Merchant SN, Eavey RD, McKenna M, Nadol JB Jr, Miyamoto RT, Linthicum FH Jr, Lubianca Neto JF et al (1998) Mutations in a novel cochlear gene cause DFNA9, a human nonsyndromic deafness with vestibular dysfunction. Nat Genet 20:299–303
2. Robertson NG, Skvorak AB, Yin Y, Weremowicz S, Johnson KR, Kovatch KA, Battey JF, Bieber FR, Morton CC (1997) Mapping and characterization of a novel cochlear gene in human and in mouse: a positional candidate gene for a deafness disorder, DFNA9. Genomics 46:345–354
3. Trexler M, Banyai L, Patthy L (2000) The LCCL module. Eur J Biochem 267:5751–5757
4. Hildebrand MS, Gandolfo L, Shearer AE, Webster JA, Jensen M, Kimberling WJ, Stephan D, Huygen PL, Smith RJ, Bahlo M (2010) A novel mutation in COCH-implications for genotype–phenotype correlations in DFNA9 hearing loss. Laryngoscope 120:2489–2493
5. Hildebrand MS, Tack D, Deluca A, Hur IA, Van Rybroek JM, McMordie SJ, Muilenburg A, Hoskinson DP, Van Camp G, Pensak ML et al (2009) Mutation in the COCH gene is associated with superior semicircular canal dehiscence. Am J Med Genet A 149A:280–285
6. Baek JI, Cho HJ, Choi SJ, Kim LS, Zhao C, Sagong BR, Kim UK, Jeong SW (2010) The Trp117Arg mutation of the *COCH* gene causes deafness in Koreans. Clin Genet 77:399–403
7. Crovetto MA, Whyte J, Sarasola E, Rodriguez JA, Garcia-Barcina MJ (2012) Absence of COCH gene mutations in patients with superior semicircular canal dehiscence. Am J Med Genet A (in press)
8. Bhattacharya SK (2006) Focus on molecules: cochlin. Exp Eye Res 82:355–356
9. Khetarpal R, Halwai G, Marwaha RK, Trehan A, Narasimhan KL, Bhalla AK (1999) Retro-peritoneal cystic lymphangioma in association with fetal hydantoin syndrome. Indian J Pediatr 66:294–297
10. Robertson NG, Hamaker SA, Patriub V, Aster JC, Morton CC (2003) Subcellular localisation, secretion, and post-translational processing of normal cochlin, and of mutants causing the sensorineural deafness and vestibular disorder, DFNA9. J Med Genet 40:479–486
11. Grabski R, Szul T, Sasaki T, Timpl R, Mayne R, Hicks B, Sztul E (2003) Mutations in COCH that result in non-syndromic autosomal dominant deafness (DFNA9) affect matrix deposition of cochlin. Hum Genet 113:406–416
12. Street VA, Kallman JC, Robertson NG, Kuo SF, Morton CC, Phillips JO (2005) A novel DFNA9 mutation in the vWFA2 domain of COCH alters a conserved cysteine residue and intrachain disulfide bond formation resulting in progressive hearing loss and site-specific vestibular and central oculomotor dysfunction. Am J Med Genet A 139A:86–95
13. Krieger E, Koraimann G, Vriend G (2002) Increasing the precision of comparative models with YASARA NOVA—a self-parameterizing force field. Proteins 47:393–402
14. Lee JO, Bankston LA, Arnaout MA, Liddington RC (1995) Two conformations of the integrin A-domain (I-domain): a pathway for activation? Structure 3:1333–1340
15. Higgins JM, Cernadas M, Tan K, Irie A, Wang J, Takada Y, Brenner MB (2000) The role of alpha and beta chains in ligand recognition by beta 7 integrins. J Biol Chem 275:25652–25664
16. Zhang L, Plow EF (1999) Amino acid sequences within the alpha subunit of integrin alpha M beta 2 (Mac-1) critical for specific recognition of C3bi. Biochemistry 38:8064–8071
17. Dickeson SK, Santoro SA (1998) Ligand recognition by the I domain-containing integrins. Cell Mol Life Sci 54:556–566
18. Bergelson JM, Hemler ME (1995) Integrin-ligand binding. Do integrins use a 'MIDAS touch' to grasp an Asp? Curr Biol 5:615–617
19. Whittaker CA, Hynes RO (2002) Distribution and evolution of von Willebrand/integrin A domains: widely dispersed domains with roles in cell adhesion and elsewhere. Mol Biol Cell 13:3369–3387
20. Eavey RD, Manolis EN, Lubianca J, Merchant S, Seidman JG, Seidman C (2000) Mutations in COCH (formerly Coch5b2) cause DFNA9. Adv Otorhinolaryngol 56:101–102
21. Lee JO, Rieu P, Arnaout MA, Liddington R (1995) Crystal structure of the A domain from the alpha subunit of integrin CR3 (CD11b/CD18). Cell 80:631–638
22. Lacy DB, Wigelsworth DJ, Scobie HM, Young JA, Collier RJ (2004) Crystal structure of the von Willebrand factor A domain of human capillary morphogenesis protein 2: an anthrax toxin receptor. Proc Natl Acad Sci U S A 101:6367–6372
23. Nagy I, Trexler M, Patthy L (2008) The second von Willebrand type A domain of cochlin has high affinity for type I, type II and type IV collagens. FEBS Lett 582:4003–4007

24. Vriend G (1990) WHAT IF: a molecular modeling and drug design program. J Mol Graph 8(52–56):29
25. Jones SM, Robertson NG, Given S, Giersch AB, Liberman MC, Morton CC (2011) Hearing and vestibular deficits in the Coch(−/−) null mouse model: comparison to the Coch(G88E/G88E) mouse and to DFNA9 hearing and balance disorder. Hear Res 272:42–48
26. Tebo AE, Szankasi P, Hillman TA, Litwin CM, Hill HR (2006) Antibody reactivity to heat shock protein 70 and inner ear-specific proteins in patients with idiopathic sensorineural hearing loss. Clin Exp Immunol 146:427–432
27. Boulassel MR, Tomasi JP, Deggouj N, Gersdorff M (2001) COCH5B2 is a target antigen of anti-inner ear antibodies in autoimmune inner ear diseases. Otol Neurotol 22:614–618
28. Baek MJ, Park HM, Johnson JM, Altuntas CZ, Jane-Wit D, Jaini R, Solares CA, Thomas DM, Ball EJ, Robertson NG et al (2006) Increased frequencies of cochlin-specific T cells in patients with autoimmune sensorineural hearing loss. J Immunol 177:4203–4210
29. Bischoff AM, Pauw RJ, Huygen PL, Aandekerk AL, Kremer H, Cremers CW, Cruysberg JR (2007) Vertical corneal striae in families with autosomal dominant hearing loss: DFNA9/COCH. Am J Ophthalmol 143:847–852